PRIMARY RESEARCH PAPER

Habitat templates of phytoplankton functional groups in tropical reservoirs as a tool to understand environmental changes

Cihelio Alves Amorim ⓘ · Ariadne do Nascimento Moura ⓘ

Abstract Trait-based classifications can efficiently capture species' responses to environmental gradients and their impacts on ecosystem functioning. Thus, the clustering of phytoplankton species into functional groups can improve the understanding of their relationships with the environment and help to predict their response to environmental changes. Accordingly, this study aimed to create habitat templates of Reynolds phytoplankton functional groups (RFGs) in tropical drinking water reservoirs to describe, explain, and predict their occurrence and formation of blooms. We analyzed the structure of RFGs in 10 tropical reservoirs, in humid and semiarid regions of Brazil, and defined their relationships with 10 environmental variables. We designated the habitat template based on niche differentiation, thresholds for the occurrences and bloom formation, cluster analyses, and generalized additive models. We identified 136 species, assembled in 20 RFGs. Six groups of habitat templates were recognized based on environmental conditions and dominant RFGs, usually represented by bloom-forming species of cyanobacteria, dinoflagellates, green algae, and diatoms. The functional groups D, X1, and P presented the most restrictive occurrences, while RFGs M and S_N displayed the widest, occurring in almost all sets of conditions. Moreover, salinity was the best predictor of RFGs' biomass (higher R^2), followed by depth, soluble reactive phosphorus, irradiance, water transparency, and dissolved inorganic nitrogen. Our approach improves the understanding of how RFGs interact with environmental gradients in tropical reservoirs, helping water managers to adopt sustainable practices to control algal blooms, based on predictions of the future state of dominance.

Keywords Assemblages · Drylands · Algal blooms · Predictive models · Salinity · Water quality

C. A. Amorim (✉) · A. d. N. Moura
Department of Biology, Graduate Program in Biodiversity, Federal Rural University of Pernambuco - UFRPE, Manoel de Medeiros Avenue, Dois IrmãosRecife, PE 52171-900, Brazil
e-mail: alvescihelio@gmail.com

A. d. N. Moura
e-mail: ariadne_moura@hotmail.com

C. A. Amorim
Department of Biological Sciences, Middle East Technical University, Üniversiteler Mahallesi, Dumlupınar Bulvarı, 60800 Ankara, Turkey

Introduction

Organisms' traits can represent their response to environmental drivers or their effects on ecosystem functioning, besides increasing the predictability of the community's response to environmental changes (Kruk et al., 2021). Thus, explaining the main processes driving plankton diversity and structure is a central question in community ecology (Hutchinson, 1961; Rojo, 2021). For phytoplankton assemblages, species coexistence is driven by several biotic and abiotic filters that affect species interactions (Borics et al., 2020). These filters influence more traits of species than species themselves, generating patterns of dominance when conditions become favourable to some species or not suitable for others (Reynolds et al., 2002).

Considering that phytoplankton is a highly diverse group of photosynthetic organisms (Borics et al., 2021), species-level classifications can often generate chaotic dynamics under certain circumstances, even after the advances in the study of physiology and ecology of the organisms (Benicà et al., 2015). To alleviate this problem, trait-based approaches and functional groups are often used to classify phytoplankton species without losing important features and responses (Reynolds et al., 2002; Salmaso & Pádisak, 2007; Kruk et al., 2010). The definition of functional groups can cluster different sets of species with common functional features that respond in a similar way to environmental changes and present the same effects on ecosystem functioning (Kruk et al., 2021).

Based on that, Reynolds (1998) and Reynolds et al. (2002) created phytoplankton functional groups (hereafter Reynolds Functional Groups – RFG, Kruk et al., 2017) to cluster species with similar tolerance and preferences and that co-occur in the same environment at the same time. These groups were created based on the habitat template, which included eight environmental variables: mixing zone depth, irradiance, water temperature, acidity and alkalinity, herbivorous zooplankton, soluble reactive phosphorus, dissolved inorganic nitrogen, and soluble reactive silica (Reynolds, 2006). Although this approach has been widely used for many years (Padisák et al., 2009; Kruk et al., 2021) and environmental conditions have been proven to be coherent with the assemblages (Salmaso et al., 2015), some groups are not well-defined in terms of habitat template and driving processes (Padisák et al.,

2009), and some new environmental factors should be further studied, e.g., salinity and the amount of the inoculum (Kruk et al., 2021).

The diversity and composition of phytoplankton are primarily controlled by local filters and biotic interactions (Borics et al., 2021). Important filters select specific attributes that act more strongly in some species or groups, creating different patterns of abundance in response to the environmental gradients (Reynolds, 1998). As predicted by the "habitat template" concept, introduced by Southwood (1977), the environment exerts influence on the fitness of the organisms, populations, or groups of species, which will select certain adaptations for better reproduction and survival (Townsend et al., 1997). This approach has been proved to be useful for classifying and predicting phytoplankton community structure without losing important information on tolerance and requirements in the natural environment (Reynolds, 1998), both for RFGs (Reynolds, 2006) and for morphology-based functional groups (Kruk & Segura, 2012).

Answering the question "what lives where and why?" (Reynolds, 1998) has been a big challenge for phytoplankton ecologists over the years. Since the proposal of classification of RFGs, much has been done towards its development, especially to describe spatial–temporal patterns in phytoplankton ("what lives where?"), but less often to explain those patterns ("why and how?"), and scarcely to predict ("when and where in new scenarios") (Kruk et al., 2021). To answer the question "what lives where", a descriptive framework aiming to describe the quantitative habitat templates where species are distributed in space and time can be followed (Reynolds, 1998). When the focus is to answer "why and how", ecologists must explain the main mechanisms driving community assembly, relationships with environmental variables, biological interactions, and ecosystem functioning. Finally, to understand "when and where in new scenarios" the focus should be on predicting future scenarios of community responses to environmental changes and effects on ecosystem functioning and services (Kruk et al., 2021).

Phytoplankton functional groups are often used in water quality assessments and algal bloom status in temperate, subtropical, and tropical lakes (e.g., Padisák et al., 2006; Crossetti et al., 2019; Braga & Becker, 2020; Long et al., 2020). Indeed, harmful

algal blooms are among the main causes of biodiversity loss and the reduction of ecosystem functioning in freshwaters (Moura et al., 2018; Reid et al., 2019; Amorim & Moura, 2021). Consequently, phytoplankton-dominated shallow lakes support fewer ecosystem services than macrophyte-dominated systems, which can impair the achievement of the United Nations Sustainable Development Goals (Janssen et al., 2021). Therefore, understanding how phytoplankton assemblages interact with environmental gradients will help water managers to improve the sustainable use of drinking water reservoirs, ensuring the provision of food, clean water and sanitation, biodiversity, climate regulation, and sustainable development.

Accordingly, in this study, we evaluated the dynamics of RFGs in a set of tropical drinking water reservoirs and created links to the relevant environmental factors driving their biomass, distribution, and bloom development. Our main goal is to establish the main RFGs and their habitat templates for tropical reservoirs, to explain and predict their presence, and even blooms, in the foreseeable new conditions. Furthermore, our approach will help water managers to predict the main impacts of algal blooms on biodiversity, water quality, ecosystem functioning, and services, besides supporting the adoption of sustainable practices.

Material and methods

Study sites, sampling, and analyses

We sampled phytoplankton from 10 tropical drinking water reservoirs in Pernambuco state, Brazil. The reservoirs presented contrasting environmental conditions, ranging from oligotrophic to hypereutrophic, and are distributed in a climatic gradient, in the humid, dry-subhumid, and semiarid zones of Brazil (Table S1). Moreover, all of them presented algal blooms at least in one sampling period (Amorim et al., 2020; Amorim & Moura, 2021). All studied reservoirs provide several ecosystem services for people, supporting the water public supply, irrigation, agriculture, fisheries, livestock, biodiversity, recreation, education, flood control, nutrient retention, primary production, climate regulation, among others.

Samples were collected five (Tapacurá and Cajueiro reservoirs) or four (other reservoirs) times a year from October 2017 to January 2019 ($n = 42$), comprising an annual cycle in each reservoir, with samples every three months in the rainy and dry seasons. All samples were collected from the deepest location of each reservoir, usually close to the dam and during the morning (08:00–12:00). Water transparency and depth (Zmax) were measured with a Secchi disk and an echo sounder, respectively. Water temperature, salinity, and pH were measured with a HANNA multiparametric probe (HI98194). Water temperature was further verified throughout the water column to establish the mixing zone depth (Zmix) (when there was a difference in the water temperature greater than 0.5 °C at each 0.5 m depth, i.e., the formation of the thermocline in stratified environments). Destratified environments presented a mixing zone depth equal to or almost reaching the sediment, demonstrating a complete mixture of the water column (Zmix:Zmax $\approx$ 1). The dissolved inorganic nitrogen (DIN) was calculated based on the sum of ammonia, nitrate, and nitrite, which were determined by the reaction with sodium hypochlorite and phenol for ammonia and cadmium reduction for nitrate and nitrite. The soluble reactive phosphorus (SRP) was analyzed by the ammonium molybdate and ascorbic acid reduction, catalyzed by antimony ions. The analyses were performed according to Strickland & Parsons (1965), Golterman et al. (1971), and Valderrama (1981).

Samples collected through surface trawls with a 25 μm mesh-size plankton net, fixed with 4% formaldehyde, were used for phytoplankton species identification following specialized literature (Prescott & Vinyard, 1982; Komárek & Fott, 1983; Komárek & Anagnostidis, 1986, 2005; Anagnostidis & Komárek, 1988; Round et al., 1990; Krammer & Lange-Berlalot, 1991; John et al., 2002; Wehr et al., 2015; among others). Subsurface samples (20 cm depth) were collected directly from the water column, preserved with 1% acetic Lugol, and analyzed in sedimentation chambers using an inverted microscope for phytoplankton quantification (Utermöhl, 1958). Phytoplankton was counted until achieving 400 organisms of the most abundant taxa and until the stabilization of the species curve (i.e., when no species was added) (Lund et al., 1958). The species' biomass (mg l^{-1}, wet weight) was determined according to Hillebrand et al. (1999) and grouped into Reynolds Functional Groups (RFGs) (Reynolds et al., 2002;

Padisak et al., 2009; Kruk et al., 2017; among others). All populations, even the rarest ones, were considered and classified into RFGs, following the recommendations of Rojo (2021).

Zooplankton was collected by filtering 100 l of water from the surface of the reservoirs with a 60 μm mesh-size plankton net; then the samples were fixed with 4% formaldehyde and analyzed in a 1 mL Sedgewick-Rafter chamber (three subsamples per sample or the entire sample) in an optical microscope. Biomass ($\mu g\,l^{-1}$, dry weight) was calculated based on regression formulas relating the bodyweight with length and width of rotifers and microcrustaceans (Ruttner-Kolisko, 1977; Dumont et al., 1975).

Calculations and data analyses

All statistical analyses were run in the statistical program R (version 4.0.5), with a significance level of $P < 0.05$ (R Core Team, 2021). Most data are presented as the mean and the standard deviation. When DIN and SRP concentrations were below approximately 100 and 10 $\mu g\,l^{-1}$, the reservoirs were considered N or P-limited (Chorus & Spijkerman, 2021), respectively. Phytoplankton RFGs with relative biomass greater than 50% of the total phytoplankton biomass were classified as dominant, while abundant species presented relative biomass greater than 5% of the total biomass. The biomass of herbivorous zooplankton was calculated as the sum of rotifers, calanoid copepods, nauplii, and cladocerans.

To designate the habitat template for each RFG, we selected seven of the eight environmental variables used by Reynolds (2006) (except soluble reactive silica): mixing zone depth, irradiance, water temperature, pH (instead of CO_2 concentration), herbivorous zooplankton biomass (instead of herbivorous zooplankton filtration rate), SRP, and DIN. We also incorporated three new variables that are important drivers of phytoplankton structure: water transparency, salinity, and depth. These factors can successfully represent the gradients of resources, energy, loss processes due to zooplankton grazing, and salinity. Mean values of each environmental variable were weighted by each RFG biomass to verify niche differentiation among the RFGs and create the habitat templates, following the assumptions of Southwood (1977). Weighted means were calculated by multiplying all values of each variable by the

biomass of a specific RFG, and then the sum of these results was divided by the sum of the biomasses in all samples. After that, we selected the minimum and maximum values of each environmental variable in the samples where each RFG reached relative biomass greater than 5%. However, in the case of any group that did not present a relative biomass > 5%, or only in one sample, we extracted the minimum and maximum values from all occurrences of this group. This approach allowed us to identify the specific range of conditions where each RFG can present higher biomasses.

To better illustrate the habitat templates, we clustered the reservoirs based on the biomass of the RFGs to select the habitats where they can coexist. For that, we constructed a non-metric multidimensional scaling (NMDS) ordination based on the Bray–Curtis distance matrix of RFGs, in the *vegan* package (Oksanen et al., 2018). We repeated this procedure with the habitat template matrix (weighted means), clustering the RFGs instead of the samples using a Euclidean distance matrix. Then, the slopes of SRP, mixing zone depth, and salinity were extracted to represent the gradients of resources, energy, and salinity, respectively, using the function *envfit*. The habitat template matrix was standardized using the *range* function, while the RFGs' biomass matrix was transformed (log(x + 1)).

Finally, generalized additive models (GAM) were used to verify the influence of each environmental factor on RFGs. This method accounts for linear and non-linear relationships between variables. The biomass of each RFG, mixing zone, irradiance, SRP, DIN, and salinity, were log(x + 1)-transformed. Model smoothing was evaluated using the estimated degree of freedom (e.d.f.), while R^2-adjusted and p-values ($P < 0.05$) indicated model fit and significance, respectively. All models were fitted using the *gam* function in the *mgcv* package (Wood, 2004, 2011).

Results

Reynolds Phytoplankton Functional Groups

A total of 136 phytoplankton taxa were identified for the 10 reservoirs studied, distributed mainly in Chlorophyta (51 spp.), Cyanobacteria (40 spp.), and

Bacillariophyta (19 spp.), while the others were classified into Dinophyta, Euglenophyta, Cryptophyta, and Chrysophyta (26 spp.). All taxa were included in 20 RFGs, of which 16 were abundant in at least one sample. The mean phytoplankton biomass varied greatly in each reservoir, ranging from 1.88 mg l^{-1} (standard deviation: $\pm$ 1.1) in Cursaí reservoir to 132.75 mg l^{-1} (standard deviation: $\pm$ 100.5) in Tapacurá reservoir (Fig. S1).

Group M was dominant in Tapacurá, Cajueiro, Carpina, Mundaú, Cursaí, and Serrinha reservoirs. Group L_O was dominant in Cachoeira, Goitá, and Mundaú, while L_M was dominant in Cajueiro, Cursaí, Serrinha, and Carpina. Serrinha reservoir also showed a dominance of the group S_N. Finally, Tabocas and Ipojuca reservoirs presented the dominance of the groups F and D, respectively. Groups C, H1, J, K, MP, P, S1, X1, X2, and Y were abundant at least in one sample ($> 5\%$), while the groups E, N_A, W1, and W2 always presented low relative biomass ($< 5\%$) (Fig. S1, Table 1).

What lives where, why, and how? Describing and explaining habitat templates of RFGs

To test niche differentiation among the RFGs and create the habitat templates, the mean values of 10 environmental variables were weighted by each RFG biomass (Table 2). The mean mixing zone depth to maximum depth ratio weighted by RFGs' biomass revealed that groups L_M, MP, S1, W2, and P usually occurred in destratified water bodies (i.e., Zmix:Zmax > 0.8), while groups D, W1, L_O, and H1 preferred stratified environments (Zmix:Zmax < 0.5). Groups D, W1, L_O, J, and Y occurred in reservoirs with low irradiance (< 400 µmol m^{-2} s^{-1}), while groups F, L_M, E, M, and MP presented higher biomass in environments with higher irradiance (> 700 µmol m^{-2} s^{-1}). Mean water temperature weighted by RFGs' biomass was lower for RFGs N_A and F (< 26 °C) and higher for RFGs L_O, X1, M, and MP (> 28 °C). Groups D, W1, H1, Y, K, S1, X2, S_N, and J were usually found in turbid waters (water transparency < 0.5 m), while groups E, F, and N_A preferred clear reservoirs (water transparency > 1.0 m). Groups D and W1 usually occurred in shallow reservoirs (< 3 m), and groups X1, E, F, L_M, and P preferred deep reservoirs (> 8 m) (Table 2).

In terms of the amount of resources, groups F and N_A were found in SRP-limited reservoirs (< 15 µg l^{-1}), while groups X1, M, MP, S1, and D presented higher biomasses in reservoirs with high SRP concentrations (> 150 µg l^{-1}). For DIN concentration, groups L_O and D occurred in DIN-limited waters (< 100 µg l^{-1}), while N_A, Y, J, H1, MP, and K showed higher biomasses under high DIN concentrations (> 300 µg l^{-1}). Regarding pH values, groups F, N_A, and E preferred neutral waters (pH 7 – 8), while all other groups were common in alkaline habitats (pH > 8). Regarding salinity, groups F, E, P, N_A, M, L_M, MP, and S_N were present in freshwater environments, showing low mean values weighted by the biomass (< 0.5 PSU); on the other hand, groups D and W1 were indicators of saline reservoirs (> 3 PSU), while the other groups were usually found in brackish waters (0.5–3 PSU). In terms of the biomass of herbivorous zooplankton, group F preferred environments with low biomass of herbivores (< 30 µg l^{-1}); on the other hand, all other groups, except X2, L_M, K, and J, presented higher biomasses in reservoirs with high herbivorous zooplankton biomass (> 100 µg l^{-1}), especially L_O (> 290 µg l^{-1}) (Table 2).

Based on the habitat template, we established the boundaries of environmental variables where RFGs can become abundant (or occur for the RFGs E, MP, N_A, W1, and W2) (Fig. 1). These boundaries can act as the thresholds where these groups can grow and present considerable biomasses. The RFGs D, X1, and P presented the most restrictive occurrences as abundant, while RFGs M and S_N displayed the widest.

The studied reservoirs were divided into six groups based on the structure of RFGs and similar environmental conditions (Figs. 2a,b). Accordingly, the RFGs were also clustered into six groups based on the means of each variable weighted by the RFG biomass, which also represented the clusters of reservoirs (Figs. 2c,d), besides the resources (SRP) (Fig. 2e), energy (mixing zone depth) (Fig. 2f), and salinity (Fig. 2g) gradients. The first axis of the NMDS separated the gradients of energy and salinity. The water transparency, irradiance, depth, and mixing zone depth increased the biomass of cluster 3 (RFGs L_M and P). Cluster 2 (RFGs F, E, and N_A) was positively correlated with water transparency, irradiance, and DIN. In the salinity gradient, cluster 6 (RFGs D and W1) was common in saline reservoirs. On the other hand, the second axis of the NMDS represented the resource

Table 1 Reynolds phytoplankton functional groups (RFGs), their mean (± standard deviation), minimum, and maximum relative biomasses in each tropical reservoir studied, and main representative species (*n* = 42). See Fig. 2 for reservoir abbreviations

Reservoir	RFG	Relative biomass (%)	Range (min–max)	Main representatives
TAP	M	80.2 (± 13.9)	61.8–94.6	*Microcystis panniformis* Komárek et al
	S1	6.3 (± 9.7)	0.4–23.4	*Anagnostidinema amphibium* (C.Agardh ex Gomont) Strunecký et al
	S$_N$	4.5 (± 2.2)	1.2–6.5	*Raphidiopsis raciborskii* (Woloszynska) Aguilera et al
	L$_O$	1.4 (± 2.3)	0.0–5.5	*Snowella lacustris* (Chodat) Komárek & Hindák
CAR	M	53.6 (± 39.6)	0.0–89.5	*Microcystis protocystis* W.B.Crow, *Microcystis aeruginosa* (Kützing) Kützing, *Microcystis botrys* Teling
	L$_M$	14.7 (± 23.9)	0.0–50.5	*Microcystis protocystis*, *Ceratium furcoides* (Levander) Langhans
	X1	13.9 (± 21.0)	1.4–45.4	*Schroederia setigera* (Schröder) Lemmermann
	J	8.7 (± 17.4)	0.0–34.9	*Scenedesmus ecornis* (Ehrenberg) Chodat
	C	3.8 (± 5.2)	0.5–11.6	*Cyclotella meneghiniana* Kützing
	S$_N$	1.5 (± 2.6)	0.1–5.4	*Raphidiopsis raciborskii*
GOI	L$_O$	98.4 (± 0.8)	97.4–99.1	*Ceratium furcoides*
CUR	L$_M$	33.2 (± 38.3)	0.0–66.9	*Microcystis protocystis*, *Ceratium furcoides*
	M	31.4 (± 36.3)	0.0–65.5	*Microcystis protocystis*
	K	8.3 (± 6.5)	1.5–16.8	*Aphanocapsa delicatissima* West & G.S.West, *Aphanocapsa elachista* West & G.S.West
	F	6.2 (± 5.0)	0.6–10.5	*Botryococcus braunii* Kützing, *Eutetramorus tetrasporus* Komárek
	P	5.1 (± 4.7)	0.8–9.3	*Aulacoseira granulata* (Ehrenberg) Simonsen
	X2	3.7 (± 4.2)	1.4–10.0	*Cryptomonas brasiliensis* A.Castro, C.E.M.Bicudo & D.Bicudo
	MP	2.6 (± 3.3)	0.5–7.5	*Gomphonema argur* Ehrenberg
	Y	2.1 (± 3.2)	0.0–6.8	*Cryptomonas ovata* Ehrenberg
	L$_O$	1.4 (± 2.6)	0.0–5.3	*Peridinium gatunense* Nygaard
	S$_N$	1.4 (± 2.5)	0.0–5.0	*Raphidiopsis raciborskii*
CAJ	M	70.6 (± 39.5)	0.0–90.2	*Microcystis aeruginosa*
	L$_M$	15.8 (± 38.2)	0.0–74.5	*Microcystis aeruginosa*, *Ceratium furcoides*
	S$_N$	3.5 (± 1.6)	1.8–5.9	*Raphidiopsis raciborskii*
	K	3.1 (± 4.0)	0.1–10.2	*Aphanocapsa delicatissima*
MUN	M	35.1 (± 17.3)	19.5–59.2	*Microcystis flos–aquae* (Wittrock) Kirchner
	S$_N$	22.1 (± 9.3)	13.3–33.6	*Raphidiopsis raciborskii*
	L$_O$	13.3 (± 24.7)	0.4–50.4	*Merismopedia tenuissima* Lemmermann
	H1	7.8 (± 6.9)	0.9–17.2	*Anabaenopsis elenkinii* V.V.Miller
	K	6.9 (± 6.4)	0.9–13.3	*Aphanocapsa delicatissima*
	J	3.7 (± 6.0)	0.4–12.7	*Pediastrum duplex* Meyen
	Y	2.7 (± 3.1)	0.0–6.0	*Gymnodinium* sp.
TAB	F	79.6 (± 23.6)	45.2–95.8	*Botryococcus braunii*
	K	7.8 (± 7.7)	0.3–15.4	*Aphanocapsa delicatissima*, *Aphanocapsa holsatica*
	M	2.7 (± 4.5)	0.0–9.3	*Microcystis aeruginosa*
	C	2.3 (± 4.2)	0.1–8.6	*Cyclotella meneghiniana*
	S1	1.5 (± 2.9)	0.0–5.8	*Planktolyngbya limnetica* (Lemmermann) Komárková–Legnerová & Cronberg
IPO	D	28.1 (± 32.3)	0.0–57.2	*Nitzschia* sp.
	K	23.2 (± 15.4)	0.9–35.4	*Aphanocapsa incerta* (Lemmermann) G.Cronberg & Komárek
	J	12.1 (± 17.6)	0.8–37.8	*Tetradesmus lagerheimii* M.J.Wynne & Guiry
	X2	9.5 (± 10.8)	0.1–20.1	*Plagioselmis lacustris* (Pascher & Ruttner) Javornicky

Table 1 continued

Reservoir	RFG	Relative biomass (%)	Range (min–max)	Main representatives
	L_O	9.0 (± 13.0)	1.4–28.4	*Ceratium furcoides, Synechocystis aquatilis* Sauvageau
	S1	4.1 (± 5.4)	0.0–12.1	*Planktolyngbya limnetica*
	M	3.9 (± 4.7)	0.0–9.2	*Microcystis aeruginosa*
	S_N	3.7 (± 3.0)	1.6–8.0	*Raphidiopsis raciborskii*
CAC	L_O	97.3 (± 1.0)	96.0–98.5	*Ceratium furcoides*
SER	S_N	33.2 (± 21.2)	7.3–59.1	*Raphidiopsis raciborskii*
	M	27.0 (± 27.1)	0.0–54.2	*Microcystis protocystis, Microcystis panniformis*
	L_M	14.2 (± 24.5)	0.0–50.9	*Microcystis panniformis, Ceratium furcoides*
	S1	8.7 (± 7.0)	4.2–19.1	*Planktolyngbya limnetica*
	P	8.6 (± 16.6)	0.0–33.5	*Aulacoseira granulata*
	H1	4.1 (± 2.8)	1.7–8.1	*Sphaerospermopsis aphanizomenoides* (Forti) Zapomelová et al

gradient, separating DIN and SRP + pH on opposite sides. Clusters 1 (RFG L_O) and 4 (RFGs S1, MP, M, and X1) were mainly positively influenced by the gradients of SRP, herbivorous zooplankton, temperature, and pH. The latter cluster was also positively influenced by depth and mixing zone. Finally, cluster 5 (RFGs Y, K, X2, J, H1, W2, C, and S_N) was influenced by moderate levels of DIN and salinity.

The six groups of reservoirs presented contrasting environmental parameters and phytoplankton communities (Fig. S2). In summary, the first group (Goitá and Cachoeira) was represented by eutrophic, deep, and stratified (low Zmix:Zmax) reservoirs, with high temperature, water transparency, and herbivorous zooplankton biomass, neutral pH, in addition to low irradiance and salinity. The second group (Tabocas) was represented by deep, mesotrophic, and stratified (low Zmix:Zmax) reservoirs, with high irradiance, water transparency, neutral pH, in addition to low herbivorous zooplankton biomass, SRP, DIN, and salinity. Similarly, the third group (Cursaí) showed oligotrophic conditions, was destratified most of the time, with high depth, irradiance, water transparency, neutral pH, low herbivorous zooplankton biomass, SRP, DIN, and salinity (Fig. S2).

The fourth group (Carpina) was hypereutrophic, deep, destratified (Zmix:Zmax = 1), with high water transparency, temperature, pH, SRP, and salinity (moderately saline), besides low herbivorous zooplankton biomass. In addition, the fifth group (Cajueiro—mesotrophic, Tapacurá, Mundaú, and Serrinha—hypereutrophic) was represented, in general, by alkaline conditions, low to moderate irradiance, low herbivorous zooplankton biomass in Mundaú and Serrinha, and high in Tapacurá and Cajueiro, low water transparency and salinity. Tapacurá presented the highest concentrations of SRP, and Mundaú had the highest concentrations of DIN. Finally, the sixth group (Ipojuca) was shallow, saline, hypereutrophic, stratified (low Zmix:Zmax), and alkaline, with low herbivorous zooplankton biomass, besides showing the lowest values of irradiance and water transparency (Fig. S2).

When and where in new scenarios? Predicting the responses of RFGs to environmental changes

Generalized additive models were useful for clearly describing the relationships among RFGs and the 10 environmental variables (Fig. 3, Figs. S3–S12, Table S2). Groups C, M, MP, S1, and S_N were positively influenced by pH, and negatively by water transparency. Furthermore, higher pH boosted the growth of groups H1, L_M, and X1, while it negatively impacted group F. Irradiance negatively impacted groups D, J, L_O, and W1, while water temperature negatively influenced groups F, K, and N_A. The herbivorous zooplankton biomass positively influenced only group L_O (Fig. 3, Figs. S3–S12, Table S2).

Table 2 The mean values of the ten environmental variables weighted by the biomass of each Reynolds' functional group (RFG) to represent the habitat template with the best conditions for their growth in the tropical reservoirs studied ($n = 42$)

RFG	Zmix (m)	Zmix:Zmax	Irradiance (μmol m^{-2} s^{-1})	Water temperature (°C)	pH	Herbivorous zooplankton (μg l^{-1})	SRP (μg l^{-1})	DIN (μg l^{-1})	Water transparency (m)	Salinity (PSU)	Depth (m)
C	3.42	0.66	482.83	27.40	8.57	149.18	85.19	187.45	0.60	1.76	4.78
D	1.16	0.49	198.50	27.93	8.85	115.88	158.34	99.69	0.20	4.39	2.36
E	5.12	0.61	833.61	27.17	7.88	112.90	74.62	103.60	1.16	0.17	8.67
F	6.23	0.74	1070.68	25.96	7.41	28.94	13.04	124.77	1.08	0.10	8.46
H1	3.05	0.59	509.36	27.69	8.72	122.51	87.54	332.57	0.40	0.83	4.79
J	3.08	0.72	347.96	27.15	8.34	85.33	53.85	360.59	0.46	1.64	4.01
K	2.47	0.71	406.06	26.50	8.56	66.07	88.75	305.61	0.44	1.92	3.50
L$_M$	7.52	0.91	869.02	26.46	8.80	62.83	92.99	166.19	0.89	0.33	8.17
L$_O$	3.57	0.59	254.14	28.70	8.30	297.92	48.61	99.57	0.95	0.70	5.88
M	5.18	0.74	776.17	28.32	8.78	148.21	259.17	199.86	0.61	0.27	7.12
MP	5.91	0.90	721.85	28.13	8.64	144.32	242.15	326.29	0.57	0.35	6.47
N$_A$	4.20	0.78	545.25	25.31	7.62	122.08	13.13	772.48	1.04	0.25	6.11
P	6.94	0.81	612.35	26.48	8.62	144.83	96.95	166.79	0.79	0.23	8.01
S1	5.62	0.86	697.23	27.70	8.82	104.34	193.06	156.44	0.44	0.73	6.27
S$_N$	4.05	0.70	566.71	27.73	8.74	108.88	84.88	224.16	0.45	0.43	5.46
W1	1.28	0.52	230.96	27.83	8.64	121.61	98.56	229.12	0.27	4.00	2.43
W2	4.32	0.82	460.85	27.85	8.69	105.22	75.55	117.48	0.87	1.31	4.98
X1	6.92	0.79	609.16	28.58	8.59	135.89	368.97	106.62	0.77	0.62	9.04
X2	2.68	0.76	400.83	26.66	8.32	61.84	35.82	131.00	0.45	1.97	3.56
Y	2.18	0.69	396.54	26.75	8.39	122.70	80.47	610.25	0.41	2.35	3.10

Variables: mixing zone depth (Zmix), mixing zone to depth ratio (Zmix:Zmax, i.e., percentage of the mixed superficial layer), irradiance, water temperature, pH, herbivorous zooplankton biomass, soluble reactive phosphorus (SRP), dissolved inorganic nitrogen (DIN), water transparency, salinity, and depth. The mixing zone to depth ratio (Zmix:Zmax) was not used for the NMDS analyses

Besides that, groups C, H1, J, K, and Y showed a significant correlation with shallow, saline, stratified (low mixing depth), and turbid conditions. Group X2 was further negatively impacted by higher water transparency. Moreover, groups D and W1 were also associated with shallow, stratified, and saline environments. Group F was associated with extremely low values of salinity (< 0.05 PSU), while group M and S$_N$ showed a positive relationship with salinity until 0.5 PSU and decreased markedly in biomass after this value; however, group S$_N$ showed a positive relationship again after 2 PSU, while group X2 presented higher biomasses at approximately 2.5 PSU. Depth further negatively influenced groups S1, S$_N$, and W2 (Fig. 3, Figs. S3–S12, Table S2).

Fig. 1 Polar area charts showing the minimum and maximum ▶ values (limits of the red bars) of the 10 environmental variables where each Reynolds functional group (RFG) can grow intensely and become abundant (relative biomass > 5%) to represent thresholds of their occurrence as abundant in the tropical reservoirs studied ($n = 42$). Groups marked with an asterisk (*) represent those that did not reach relative biomass > 5%, or did it only in one sample, so, the limits represent the thresholds of their occurrence. Variables: mixing zone depth, irradiance, water temperature, pH, biomass of herbivorous zooplankton, soluble reactive phosphorus (SRP), dissolved inorganic nitrogen (DIN), water transparency, salinity, and depth

Concentrations of DIN positively influenced only groups N$_A$ and Y. Concentrations of SRP positively influenced groups M, MP, S1, and X1, besides
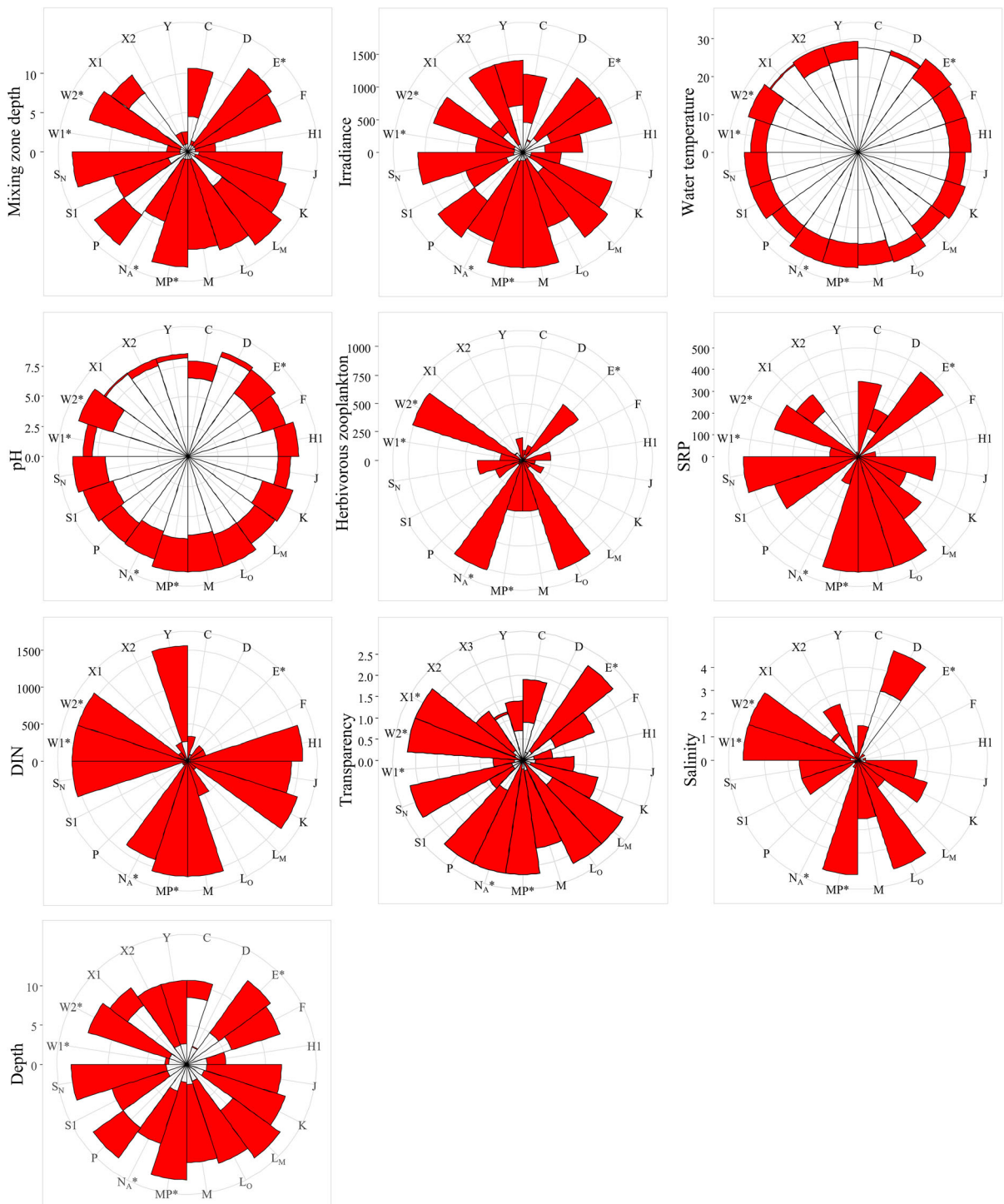
showing an opposite relationship with groups E and F.
The SRP also increased the biomass of groups D and
W2 until concentrations of approximately 100 μg L^{-1}

showing an opposite relationship with groups E and F.
The SRP also increased the biomass of groups D and
W2 until concentrations of approximately 100 μg L^{-1}

and negatively impacted them at extreme values. Only
group P did not correlate with any of the environmen-
tal variables (Fig. 3, Figs. S3–S12, Table S2).

In general, salinity was the best predictor of the RFGs' biomass (higher R^2), accounting for 98.8% of the variance of the RFG D, 92% for X2, 89.2% for W1, 78.3% for K, 72.4% for F, 61.3% for C, and 48.6% for Y. Depth was the second-best predictor (60.6% for K, 51.6% for Y, 36.5% for C, and 33.7% for J), followed by SRP (51.9% for E, 39% for X1, and 36.9% for W2), irradiance (37.6% for D), water transparency (37.5% for S1, and 31.4% for S_N), and DIN (34.7% for Y). Mixing depth, water temperature, herbivorous zooplankton, and pH always explained less than 30% of the variance in each RFG's biomass (Fig. 3, Figs. S3–S12, Table S2).

Discussion

What lives where, why, and how? Habitat template and driving processes

The habitat template of most RFGs was constructed primarily based on samples from the temperate region. When this classification was proposed, much less information was available for tropical regions (e.g., Reynolds, 1998, 2006; Reynolds et al., 2002). More recently, Salmaso et al. (2015) graphically represented the habitat template of the RFGs based on data from Reynolds et al. (2002). They statistically confirmed the relationships of the RFGs with environmental variables. However, more information about tropical habitats is needed. Accordingly, in this study, we defined the habitat template for 20 RFGs in tropical drinking water reservoirs, describing the main environmental conditions where they are most successful and can form blooms. Moreover, we designated the boundaries of 10 environmental variables where RFGs can become dominant in tropical reservoirs. These boundaries can act as assembly rules of phytoplankton, delimiting the limits of their occurrences. According to Keddy & Weiher (1999), assembly rules are "values and domain of factors that either structure or constrain the properties of ecological assemblages". So, those rules must be explicit and quantitative values of key factors, instead of merely describing a pattern (Keddy & Weiher, 1999; Rojo, 2021), as the most descriptive studies did until now.

In our approach, we classified all phytoplankton populations into RFGs, even the non-abundant ones (relative biomass < 5%), unlike most studies (e.g.,

Costa et al., 2016; Rodrigues et al., 2018; Braga & Becker, 2020; Kruk et al., 2021). Non-dominant species can act as the inoculum of the future assemblages, because, even at low biomasses, they can compete for resources better than dominant species under certain circumstances (Rojo & Álvarez-Cobelas, 2003). Thus, they must not be underestimated (Rojo, 2021). Nevertheless, how the input of a new inoculum affects phytoplankton assembly has not been evaluated yet (Kruk et al., 2021). By considering abundant and non-abundant groups, our approach is also useful for predicting how environmental changes will affect the structure of future phytoplankton assemblages, and thus researchers can estimate when and where phytoplankton RFGs will be more successful under new scenarios of global change.

From the 20 RFGs identified in our study, groups E, N_A, W1, and W2 did not present enough biomass to be considered abundant. However, they were present in unique conditions that allowed their growth and tolerance to environmental pressures. If these conditions become more intense, these groups will probably present their best fitness, achieving higher biomasses and possibly becoming dominant in future assemblages. Moreover, what defines the successful development of a phytoplankton species is not its biomass, but how it tolerates environmental inadequacies when it arrives in a new habitat (Reynolds, 2012). Accordingly, evaluating the habitat template and environmental drives of non-dominant groups or species is important in predicting the state and structure of future assemblages.

Based on that, we were able to separate the reservoirs into six main groups of habitat templates. These clusters better reflected the environmental conditions, as well as the RFGs they hosted and their responses to the resource, energy, and salinity gradients. This is the first attempt to recreate the habitat templates of RFGs since their proposal and based on new data. Previously to this article, Salmaso et al. (2015) statistically illustrated the environmental tolerances of 30 RFGs using data from Reynolds' experiments in temperate lakes. They clustered RFGs into five groups, which were distributed in two main gradients of tolerance: temperature/grazing + DIN, and SRP/irradiance + carbon dioxide. Moreover, the tolerances to low mixing depth and silica concentration were not related to RFG patterns (Salmaso et al., 2015). Even being based on environmental
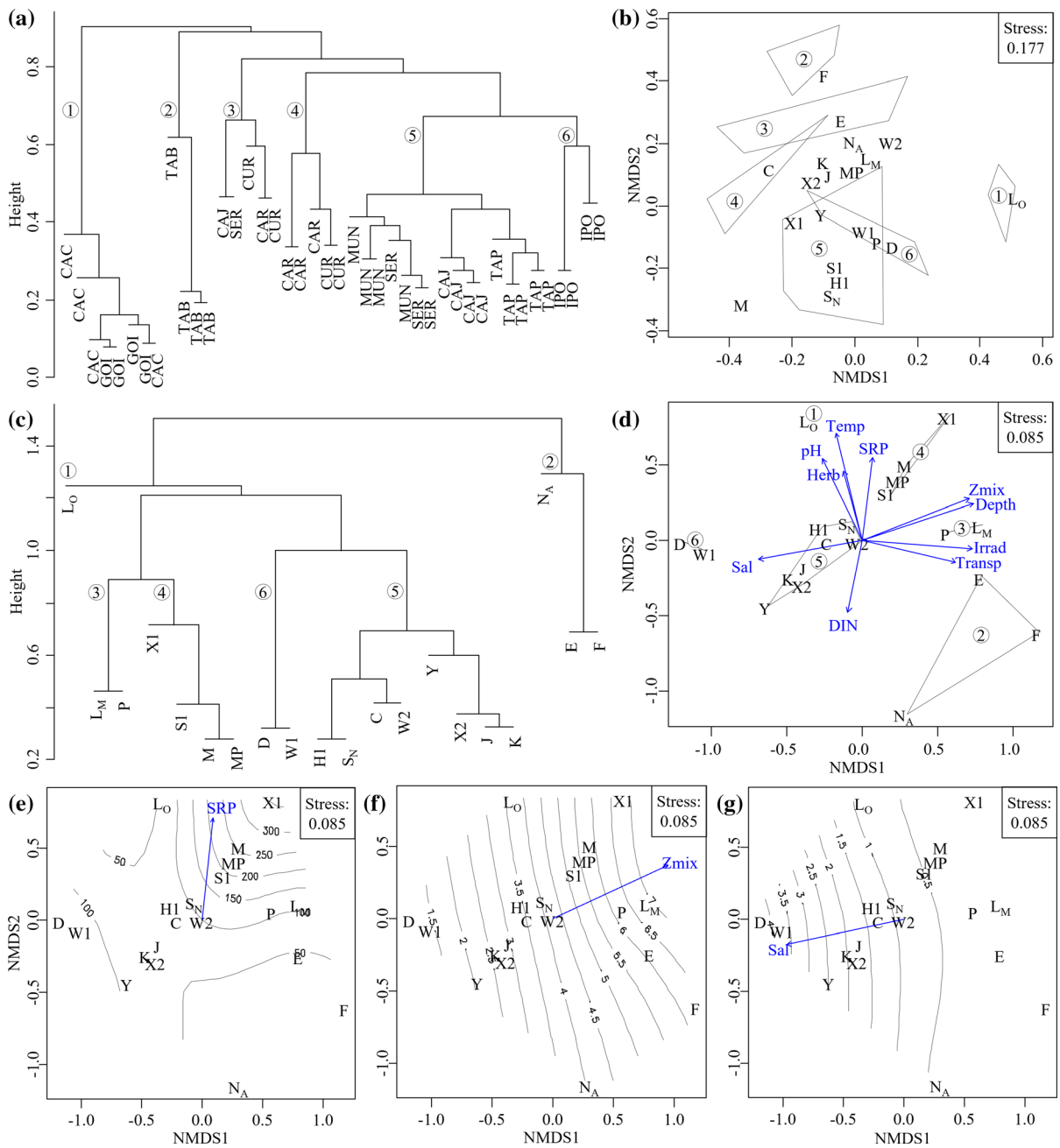
Fig. 2 Bray–Curtis dissimilarity analysis (**a**) and Non-metric multidimensional scaling (NMDS) ordination (**b**) showing the clustering reservoirs based on the biomass of Reynolds functional groups (RFG) ($n = 42$). Euclidean distance analysis (**c**) and NMDS ordination (**d**) of the habitat templates (means of variables weighted by the biomass of each RFG) and their relationships with the environmental variables in the tropical reservoirs studied ($n = 20$). Panels (**e**), (**f**), and (**g**) show the distribution of each RFG along the gradients of resources (SRP), energy (mixing zone depth), and salinity, respectively. Variables: mixing zone depth (Zmix), irradiance (Irrad), water temperature (Temp), pH, the biomass of herbivorous zooplankton (Herb), soluble reactive phosphorus (SRP), dissolved inorganic nitrogen (DIN), water transparency (Transp), and salinity (Sal). Clusters of reservoirs: 1—Goitá (GOI) and Cachoeira (CAC); 2—Tabocas (TAB); 3—Cursaí (CUR); 4—Carpina (CAR); 5—Tapacurá (TAP), Mundaú (MUN), Serrinha (SER), and Cajueiro (CAJ); 6—Ipojuca (IPO)
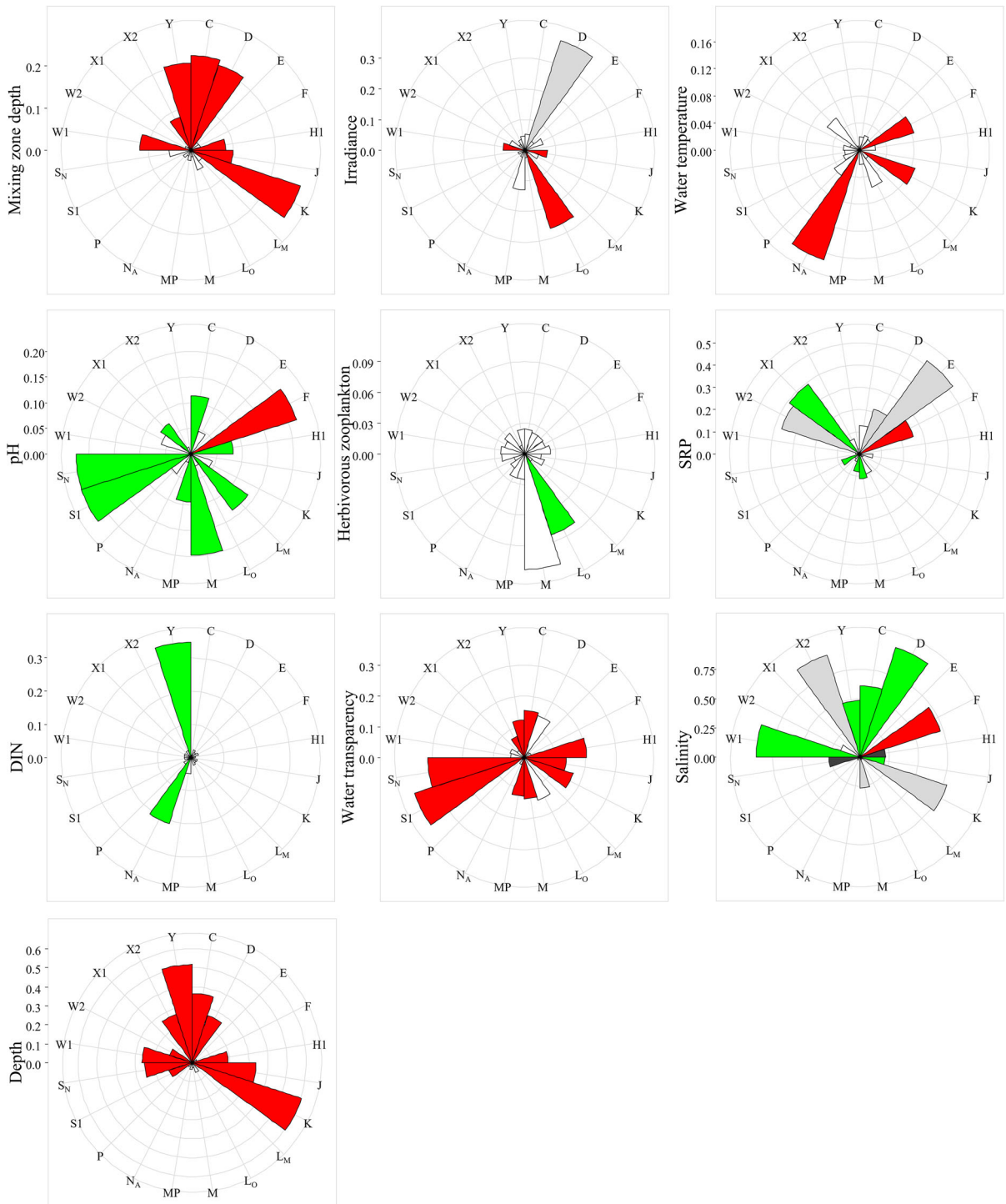
◀ **Fig. 3** Polar area charts showing the strength of the influence of the 10 environmental variables on each Reynolds functional group (RFG) in the tropical reservoirs studied ($n = 42$), assessed by the R^2-adjusted from generalized additive models—GAM. Variables: mixing zone depth, irradiance, water temperature, pH, the biomass of herbivorous zooplankton, soluble reactive phosphorus (SRP), dissolved inorganic nitrogen (DIN), water transparency, salinity, and depth. Green bars: positive influence; red bars: negative influence; dark grey bars: humped-type relationship with the main influence negative and then positive; light grey bars: humped-type relationship with the main influence positive and then negative; white bars: non-significant relationships

preferences (weighted means of environmental variables) instead of tolerance levels, our analyses revealed different gradients that regulated the patterns of phytoplankton assemblages in tropical reservoirs (resource: DIN/SRP + pH, and energy/salinity gradients).

In the resource gradient, clusters 1 (RFG L_O) and 4 (RFGs S1, MP, M, and X1) were associated with alkaline, SRP-rich, and DIN-deficient waters, while cluster 2 (RFGs N_A, E, F) correlated with higher concentrations of DIN, lower SRP and neutral pH. In the energy/salinity gradient, clusters 2 and 3 (RFGs L_M and P) were related to deep and destratified freshwaters, with high transparency and irradiance. The opposite was found for cluster 6 (RFGs D and W1), which was related to shallow, saline, turbid, and stratified waters with low irradiance. Although cluster 5 (RFGs Y, X2, K, J, C, H1, W2, and S_N) was placed at the centre of the NMDS, it tended to be associated with moderate salinities and DIN concentrations. Herbivorous zooplankton and temperature showed a lower influence on RFG structure, but they were important to explain the occurrence of the RFGs L_O and N_A, respectively. The lower influence of these variables on phytoplankton assembly had already been demonstrated for tropical reservoirs. Considering that zooplankton communities from tropical lakes and reservoirs are usually represented by small organisms (Ger et al., 2016; Amorim et al., 2019), they present lower effects on phytoplankton assemblages (Amorim & Moura, 2020; Amorim et al., 2020), which are in turn well adapted to prevent for being grazed by zooplankton (Wilson et al., 2006).

In contrast to the results found by Salmaso et al. (2015), our habitat template representation, associated with GAM models, showed a stronger effect for

mixing zone depth than temperature. This can represent an important difference between tropical and temperate climates. Due to warmer climates, tropical lakes tend to be stratified for longer periods (Brasil et al., 2016), but with similar temperatures throughout the year (Kosten et al., 2009), which can reduce the effects of temperature on phytoplankton assemblages and increase the contribution of stratification in tropical lakes and reservoirs (Amorim et al., 2020).

Furthermore, we also registered the inverse influence of DIN and SRP on phytoplankton assemblages, which can also be a climate-related effect that differs from Salmaso et al. (2015). For instance, higher temperatures, and consequent stratification, can induce a higher release of phosphorus from the sediments, especially in shallow lakes (Jeppesen et al., 2020). On the other hand, the denitrification processes, and consequent loss of nitrogen, are higher with rising temperatures (Herrman et al., 2008). So, considering that the SRP gradient was coupled with temperature in the NMDS analysis, higher concentrations of SRP, associated with low values of DIN, are expected for tropical lakes and reservoirs.

Salinity was the main predictor of ecological changes in phytoplankton assemblages in the reservoirs studied herein. Although salinity has been recognized as one of the main drivers of aquatic organisms in warmer regions, especially in drylands (Barbosa et al., 2020), it was not considered in the original proposal of RFGs' habitat templates (Kruk et al., 2021). Until certain levels, it is recognized that salinity can stimulate cyanobacterial blooms (Amorim et al., 2020), which can coexist with other phytoplankton assemblages, including diatoms, dinoflagellates, and green algae; and thus, reducing water quality, biodiversity, and ecosystem functioning (Amorim & Moura, 2021). So, it is also important to further study the effects of salinity on phytoplankton in large gradients, capturing the main effects on community assembly and ecosystem functioning.

Additionally, we were able to redraw the habitat templates of 20 RFGs with data exclusively from the tropical region and after the inclusion of three new environmental variables (Fig. 4, Table 3). Most of the habitat templates proposed in this study match with the original description of those proposed by Reynolds (Reynolds, 1998, 2006; Reynolds et al., 2002; Padisák et al., 2009). The exceptions are: RFG E and X1, which were registered mostly in deep reservoirs
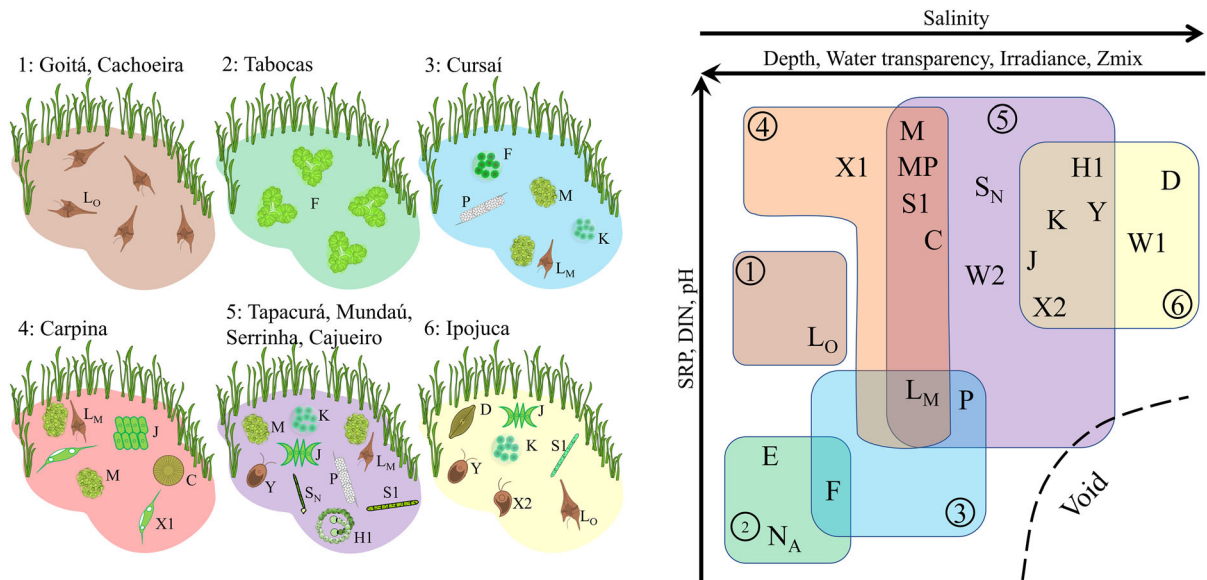
Fig. 4 Representation of the habitat templates where the 20 Reynolds functional groups (RFGs) are more successful in tropical reservoirs. The RFGs were plotted based on the resource (y-axis: soluble reactive phosphorus—SRP, dissolved inorganic nitrogen—DIN, and pH), energy (x-axis: mixing zone depth, water transparency, and irradiance), and salinity (x-axis) gradients. See results for a description of the main environmental conditions in each group of reservoirs

(instead of shallow); RFG H1, which was abundant in nitrogen-rich waters (instead of nitrogen-limited); RFG P was registered in oligotrophic to hypereutrophic reservoirs (instead of only eutrophic); and RFG L_M, that presented higher biomass in oligotrophic to hypereutrophic conditions (instead of eutrophic to hypereutrophic) (Table 3).

The RFG L_M was recognized as in an intermediate trophic state group between L_O and M (Padisák et al., 2009); however, in this study, L_M and M occurred as abundant in oligotrophic to hypereutrophic reservoirs, while L_O occurred in mesotrophic to hypereutrophic waters. According to Reynolds (2006), RFG L_M tolerates stratification and is sensitive to mixing; nevertheless, in our study, this group was present usually in deep destratified reservoirs, while L_O occurred in warm stratified waters. This result can be explained by the lower relative biomass of *Ceratium furcoides* (Levander) Langhans in *Microcystis*-dominated systems (always < 10%, except in one sample from Cursaí reservoir), which might suggest that RFG L_M is more related to M, instead of being an intermediate between L_O and M in tropical lakes and reservoirs. Likewise, *Ceratium* and *Microcystis* showed different dominance patterns in another tropical Brazilian lake, the Garças Pond, without

stable coexistence (mandatory to recognize the L_M assemblage) (Crossetti et al., 2019). So, more research is needed to verify if *Ceratium* and *Microcystis* can coexist in tropical lakes, or if this pattern is seen only in temperate and subtropical environments.

When and where in new scenarios? RFGs as predictors of environmental change

Since its proposal, the RFG approach has been largely used to describe spatiotemporal patterns of phytoplankton and its tolerance and sensitivity to environmental variables (Salmaso et al., 2015). However, much less has been done to explain "why and how" phytoplankton is assembled, and more research should focus on explaining "when and where" phytoplankton RFGs will dominate under new scenarios of environmental change (Kruk et al., 2021).

Two main modelling approaches can be used to predict phytoplankton dynamics and bloom formation, which include process-based and data-driven models (Rousso et al., 2020). Currently, PROTECH (Phytoplankton RespOnses To Environmental CHange) is one of the most common models used to predict phytoplankton structure, allowing the simulation of daily changes in the biomass of different taxa

Table 3 Comparison between the original habitat templates of 20 Reynolds Functional Groups (Reynolds et al., 2002; Padisák et al., 2009) and the habitat templates proposed in this study for the epilimnion of tropical lakes and reservoirs

RFGs	Original habitat templates (from Padisák et al. 2009)	Habitat templates for tropical lakes and reservoirs
C	Eutrophic small- and medium-sized lakes with species sensitive to the onset of stratification	Mesotrophic to hypereutrophic, stratified and destratified lakes and reservoirs
D	Shallow turbid waters including rivers	Hypereutrophic, shallow, stratified, turbid, light-limited, phosphorus-rich, nitrogen-limited, alkaline, saline lakes and reservoirs
E	Usually small, shallow, base poor lakes or heterotrophic ponds	Oligotrophic to hypereutrophic, deep, clear, with good light conditions, freshwater lakes and reservoirs
F	Clear, deeply mixed meso-eutrophic lakes	Oligotrophic to mesotrophic, deep, clear, with good light conditions, phosphorus-limited, with low biomass of herbivorous zooplankton, freshwater lakes and reservoirs
H1	Eutrophic, both stratified and shallow lakes with low nitrogen content	Hypereutrophic, shallow, stratified, turbid, nitrogen-rich, alkaline lakes and reservoirs
J	Shallow, mixed, highly enriched systems (including many low-gradient rivers)	Hypereutrophic, turbid, light-limited, nitrogen-rich, alkaline lakes and reservoirs
K	Shallow, nutrient-rich water columns	Mesotrophic to hypereutrophic, clear to turbid, with good light conditions, nitrogen-rich lakes and reservoirs
L_M	Eutrophic to hypertrophic, small- to medium-sized lakes	Oligotrophic to hypereutrophic, deep, destratified, alkaline, freshwater lakes and reservoirs
L_O	Deep and shallow, oligo to eutrophic, medium to large lakes	Mesotrophic to hypereutrophic, shallow and deep, stratified, warm, light-limited, nitrogen-limited, with high biomass of herbivorous zooplankton lakes and reservoirs
M	Eutrophic to hypertrophic, small- to medium-sized water bodies	Oligotrophic to hypereutrophic, stratified and destratified, warm, with good light conditions, phosphorus-rich, alkaline, freshwater lakes and reservoirs
MP	Frequently stirred up, inorganically turbid shallow lakes	Hypereutrophic, destratified, warm, with good light conditions, phosphorus-rich, nitrogen-rich, freshwater lakes and reservoirs
N_A	Oligo-mesotrophic, atelomictic environments at lower latitudes with species sensitive to destratification	Oligotrophic to mesotrophic, stratified and destratified, clear, phosphorus-limited, nitrogen-rich, freshwater lakes and reservoirs
P	Continuous or semi-continuous mixed layer of 2–3 m in thickness in eutrophic lakes	Oligotrophic to hypereutrophic, deep, destratified, freshwater lakes and reservoirs
S1	Turbid mixed environments	Mesotrophic to hypereutrophic, destratified, turbid, phosphorus-rich, alkaline lakes and reservoirs
S_N	Warm mixed environments	Mesotrophic to hypereutrophic, turbid, alkaline, freshwater lakes and reservoirs
W1	Ponds, even temporary, rich in organic matter from husbandry or sewages	Hypereutrophic, shallow, stratified, turbid, light-limited, alkaline, saline lakes and reservoirs
W2	Meso-eutrophic ponds, even temporary, shallow lakes	Mesotrophic to hypereutrophic, destratified, alkaline lakes and reservoirs
X1	Shallow, eu-hypertrophic environments	Hypereutrophic, deep, warm, phosphorus-rich, alkaline, brackish lakes and reservoirs
X2	Shallow, meso-eutrophic environments	Oligotrophic to hypereutrophic, turbid, alkaline lakes and reservoirs
Y	Almost all lentic ecosystems when grazing pressure is low	Oligotrophic to hypereutrophic, turbid, light-limited, alkaline lakes and reservoirs

(Reynolds et al., 2001; Elliott, 2021). However, these models require many variables and a huge dataset, which are not always available. Alternatively, data-driven models can be useful for predicting phytoplankton response to changes in environmental conditions based on a preexistent dataset (Rousso et al.,

2020). As shown above, in our study, GAM models (a data-driven approach) were efficient in predicting the response of 20 RFGs to 10 environmental gradients, providing explanations of the mechanisms involved in their dominance in specific ranges of environmental conditions (habitat templates). Based on that, we quantified the relationships between RFGs' biomass and each environmental variable for dominant, abundant, and non-abundant groups, which enabled the prediction of the most favourable set of environmental conditions considered optimal for their growth in the resource, energy, and salinity gradients (Fig. 6).

Accordingly, the ability of RFGs to predict environmental change can support the adoption of sustainable practices to avoid eutrophication. In this regard, the knowledge of the key functional traits of dominant phytoplankton groups is essential for the success of management strategies to control algal blooms (Ibelings et al., 2016). Based on that, Mantzouki et al. (2016) developed a schematic framework to inform lake managers of the best practices to control the main RFGs responsible for harmful cyanobacterial blooms. The combination of these practices will maintain the provision of ecosystem services in lakes and reservoirs, allowing the sustainable development and conservation of aquatic resources. Coupled with the information about habitat templates, those management strategies can be helpful to understand and control algal blooms in tropical drinking water reservoirs, where they are supposed to impact water quality, plankton diversity, structure, and ecosystem functioning (Amorim & Moura, 2021).

Conclusions

To the best of our knowledge, this is the first attempt to recreate the habitat template of RFGs exclusively for tropical aquatic ecosystems. We successfully designated six sets of habitat templates, based on the common RFGs and the environmental conditions where they are most successful. Furthermore, generalized additive models were useful for explaining and predicting the structure of phytoplankton, with most of the variance in the RFGs' biomass explained by salinity, depth, SRP, irradiance, transparency, and DIN. As our sampling included only the superficial layer of the reservoirs, the habitat templates proposed here should be considered only for epilimnetic phytoplankton assemblages.

Our approach does not substitute the habitat templates proposed by Reynolds et al. (2002) and Padisák et al. (2009) but complements the understanding of how RFGs interact with environmental gradients in tropical reservoirs, by considering dominant and non-dominant groups and including three new environmental variables. Based on our results, water managers can predict in which circumstances RFGs will become dominant in tropical drinking water lakes and reservoirs. With this knowledge, it will be possible to anticipate the need for restoration measures. Although we described the structure of RFGs, their main processes, and mechanisms in six sets of habitat templates, some of them are under-represented and still need further clarifications. As Reynolds (2006) said: "*the ecology of populations and communities is relevant to many aspects of human existence, from the safety of drinking water to the sustainability of fisheries. The accumulated knowledge is both broad and deep but it is far from complete*". So, more research is needed, especially to explain and predict phytoplankton structure in tropical habitats, including lakes, reservoirs, rivers, estuaries, and oceans.

Author Contributions CAA participated in the conceptualization, methodology development, validation, data curation, and formal analysis of all data, wrote the original draft, wrote, reviewed, and edited the final version of the manuscript. ANM participated in the conceptualization, supervision, funding acquisition, methodology of all data, wrote, reviewed, and edited the final version of the manuscript. All authors read and approved the final manuscript.

Declarations

Ethical approval   Not applicable.

Consent to participate Not applicable.

Consent for publication Not applicable.

Availability of data and materials The datasets used and/or analyzed during the current study are available from the corresponding author on reasonable request.

Code availability Not applicable.

References

Amorim, C. A. & A. N. Moura, 2020. Effects of the manipulation of submerged macrophytes, large zooplankton, and nutrients on a cyanobacterial bloom: A mesocosm study in a tropical shallow reservoir. Environmental Pollution 265: 114997.

Amorim, C. A. & A. N. Moura, 2021. Ecological impacts of freshwater algal blooms on water quality, plankton biodiversity, structure, and ecosystem functioning. Science of The Total Environment 758: 143605.

Amorim, C. A., C. R. Valença, R. H. Moura-Falcão & A. N. Moura, 2019. Seasonal variations of morpho-functional phytoplankton groups influence the top-down control of a cladoceran in a tropical hypereutrophic lake. Aquatic Ecology 53: 453–464.

Amorim, C. A., Ê. W. Dantas & A. N. Moura, 2020. Modeling cyanobacterial blooms in tropical reservoirs: The role of physicochemical variables and trophic interactions. Science of The Total Environment 744: 140659.

Anagnostidis, K. & J. Komárek, 1988. Modern approach to the classification system of cyanophytes. 3 – Oscillatoriales. Algological Studies/Archiv für Hydrobiologie 50/53: 327–472.

Barbosa, L. G., C. A. Amorim, G. Parra, J. Laço Portinho, M. Morais, E. A. Morales & R. F. Menezes, 2020. Advances in limnological research in Earth's drylands. Inland Waters 10: 429–437.

Benincà, E., B. Ballantine, S. P. Ellner & J. Huisman, 2015. Species fluctuations sustained by a cyclic succession at the edge of chaos. Proceedings of the National Academy of Sciences 112: 6389–6394.

Borics, G., A. Abonyi, N. Salmaso & R. Ptacnik, 2021. Freshwater phytoplankton diversity: models, drivers and implications for ecosystem properties. Hydrobiologia 848: 53–75.

Borics, G., V. B. Béres, I. Bácsi, B. A. Lukács, E. T. Krasznai, Z. Botta-Dukát & G. Várbíró, 2020. Trait convergence and trait divergence in lake phytoplankton reflect community assembly rules. Scientific Reports 10: 19599.

Braga, G. G. & V. Becker, 2020. Influence of water volume reduction on the phytoplankton dynamics in a semi-arid man-made lake: A comparison of two morphofunctional approaches. Anais Da Academia Brasileira De Ciências Academia Brasileira De Ciências 92: 20181102.

Brasil, J., J. L. Attayde, F. R. Vasconcelos, D. D. F. Dantas & V. L. M. Huszar, 2016. Drought-induced water-level

reduction favors cyanobacteria blooms in tropical shallow lakes. Hydrobiologia 770: 145–164.

Chorus, I. & E. Spijkerman, 2021. What Colin Reynolds could tell us about nutrient limitation, N: P ratios and eutrophication control. Hydrobiologia 848: 95–111.

Costa, M. R. A., J. L. Attayde & V. Becker, 2016. Effects of water level reduction on the dynamics of phytoplankton functional groups in tropical semi-arid shallow lakes. Hydrobiologia Springer 778: 75–89.

Crossetti, L. O., D. C. Bicudo, L. M. Bini, R. B. Dala-Corte, C. Ferragut & C. E. M. Bicudo, 2019. Phytoplankton species interactions and invasion by Ceratium furcoides are influenced by extreme drought and water-hyacinth removal in a shallow tropical reservoir. Hydrobiologia 831: 71–85.

Dumont, H. J., I. Van de Velde & S. Dumont, 1975. The dry weight estimate of biomass in a selection of Cladocera, Copepoda and Rotifera from the plankton, periphyton and benthos of continental waters. Oecologia 19: 75–97.

Elliott, J. A., 2021. Modelling lake phytoplankton communities: recent applications of the PROTECH model. Hydrobiologia 848: 209–217.

Ger, K. A., P. Urrutia-Cordero, P. C. Frost, L.-A. Hansson, O. Sarnelle, A. E. Wilson & M. Lürling, 2016. The interaction between cyanobacteria and zooplankton in a more eutrophic world. Harmful Algae 54: 128–144.

Golterman, H. L., R. S. Clymo & M. A. H. Ohnstad, 1971. Chemical analysis of fresh waters, Blackwell Scientific Publishers, Oxford:

Herrman, K. S., V. Bouchard & R. H. Moore, 2008. Factors affecting denitrification in agricultural headwater streams in Northeast Ohio, USA. Hydrobiologia 598: 305–314.

Hillebrand, H., C.-D. Dürselen, D. Kirschtel, U. Pollingher & T. Zohary, 1999. Biovolume calculation for pelagic and benthic microalgae. Journal of Phycology 35: 403–424.

Hutchinson, G. E., 1961. The paradox of the plankton. The American Naturalist 95: 137–145.

Ibelings, B. W., M. Bormans, J. Fastner & P. M. Visser, 2016. CYANOCOST special issue on cyanobacterial blooms: synopsis – a critical review of the management options for their prevention, control and mitigation. Aquatic Ecology 50: 595–605.

Janssen, A. B. G., S. Hilt, S. Kosten, J. J. M. Klein, H. W. Paerl & D. B. Van de Waal, 2021. Shifting states, shifting services: linking regime shifts to changes in ecosystem services of shallow lakes. Freshwater Biology 66: 1–12.

Jeppesen, E., D. E. Canfield, R. W. Bachmann, M. Søndergaard, K. E. Havens, L. S. Johansson, T. L. Lauridsen, T. Sh, R. P. Rutter, G. Warren, G. Ji & M. V. Hoyer, 2020. Toward predicting climate change effects on lakes: a comparison of 1656 shallow lakes from Florida and Denmark reveals substantial differences in nutrient dynamics, metabolism, trophic structure, and top-down control. Inland Waters 10: 197–211.

John, D. M., B. A. Whitton & A. J. Brook, 2002. The Freshwater Algal Flora of the British Isles, Cambridge University Press, Cambridge.

Keddy, P. & E. Weiher, 1999. The scope and goals of research on asssembly rules. In Weiher, E. & P. Keddy (eds), Ecological Assembly Rules: Perspectives, Advances, Retreats Cambridge University Press, Cambridge: 1–20.

Komárek, J. & B. Fott, 1983. Chlorophyceae: Chlorococcales, Begründent von August Thienemann, Stuttgart.

Komárek, J. & K. Anagnostidis, 1986. Modern approach to the classification system of Cyanophytes, 2: Chroococcales. Algological Studies/archiv Für Hydrobiologie 73: 157–226.

Komárek, J. & K. Anagnostidis, 2005. Cyanoprokayota 2: Oscillatoriales. In Budel, B., L. Krienitz, G. Gartner & M. Schargerl (eds), Süßwasserflora von Mitteleuropa Elsevier, Müncher: 1–759.

Kosten, S., V. L. M. Huszar, N. Mazzeo, M. Scheffer, L. S. L. Sternberg & E. Jeppesen, 2009. Lake and watershed characteristics rather than climate influence nutrient limitation in shallow lakes. Ecological Applications 19: 1791–1804.

Krammer, K. & H. Lange-Bertalot, 1991. Bacillariophyceae: Achnanthaceae. Kritische Ergänzungen zu *Navicula* (Lineolatae) und *Gomphonema*. In Ettl, H., G. Gärtner, J. Gerloff, H. Heynig & D. Mollenhauer (eds), Süßwasserflora von Mitteleuropa Gustav Fischer Verlag, Stuttgart: 1–486.

Kruk, C. & A. M. Segura, 2012. The habitat template of phytoplankton morphology-based functional groups Phytoplankton responses to human impacts at different scales. Hydrobiologia 698: 191–202.

Kruk, C., M. Devercelli & V. L. Huszar, 2021. Reynolds Functional Groups: a trait-based pathway from patterns to predictions. Hydrobiologia 848: 113–129.

Kruk, C., M. Devercelli, V. L. M. Huszar, E. Hernández, G. Beamud, M. Diaz, L. H. S. Silva & A. M. Segura, 2017. Classification of Reynolds phytoplankton functional groups using individual traits and machine learning techniques. Freshwater Biology 62: 1681–1692.

Kruk, C., V. L. H. Huszar, E. T. H. M. Peeters, S. Bonilla, L. Costa, M. Lürling, C. S. Reynolds & M. Scheffer, 2010. A morphological classification capturing functional variation in phytoplankton. Freshwater Biology 55: 614–627.

Long, S., T. Zhang, J. Fan, C. Li & K. Xiong, 2020. Responses of phytoplankton functional groups to environmental factors in the Pearl River, South China. Environmental Science and Pollution Research 27: 42242–42253.

Lund, J. W. G., C. Kipling & E. D. Le Cren, 1958. The inverted microscope method of estimating algal numbers and the statistical basis of estimations by counting. Hydrobiologia 11: 143–170.

Mantzouki, E., P. M. Visser, M. Bormans & B. W. Ibelings, 2016. Understanding the key ecological traits of cyanobacteria as a basis for their management and control in changing lakes. Aquatic Ecology 50: 333–350.

Moura, A. N., N. K. C. Aragão-Tavares & C. A. Amorim, 2018. Cyanobacterial blooms in freshwaters bodies in a semiarid region, northeastern Brazil: a review. Journal of Limnology 77: 179–188.

Oksanen, J., F. G. Blanchet, M. Friendly, R. Kindt, P. Legendre, D. McGlinn, P. R. Minchin, R. B. O'Hara, G. L. Simpson, P. Solymos, M. H. H. Stevens, E. Szoecs, & H. Wagner, 2018. vegan: Community Ecology Package. R Package Version 2.5–2. https://CRAN.R-project.org/package=vegan

Padisák, J., G. Borics, I. Grigorszky & É. Soróczki-Pintér, 2006. Use of phytoplankton assemblages for monitoring ecological status of lakes within the water framework directive: The assemblage index. Hydrobiologia 553: 1–14.

Padisák, J., L. O. Crossetti & L. Naselli-Flores, 2009. Use and misuse in the application of the phytoplankton functional classification: a critical review with updates. Hydrobiologia 621: 1–19.

Prescott, G. W. & W. C. Vinyard, 1982. A Synopsis of North American Desmids, University of Nebraska Press, Nebraska.

R Core Team. 2021. R: A language and environment for statistical computing. R Foundation for Statistical Computing, Vienna. https://www.R-project.org/

Reid, A. J., A. K. Carlson, I. F. Creed, E. J. Eliason, P. A. Gell, P. T. J. Johnson, K. A. Kidd, T. J. MacCormack, J. D. Olden, S. J. Ormerod, J. P. Smol, W. W. Taylor, K. Tockner, J. C. Vermaire, D. Dudgeon & S. J. Cooke, 2019. Emerging threats and persistent conservation challenges for freshwater biodiversity. Biological Reviews 94: 849–873.

Reynolds, C. S., 1998. What factors influence the species composition of phytoplankton in lakes of different trophic status? Hydrobiologia 369: 11–26.

Reynolds, C. S., 2006. Ecology of Phytoplankton, Cambridge University Press, Cambridge.

Reynolds, C. S., 2012. Environmental requirements and habitat preferences of phytoplankton: chance and certainty in species selection. Botanica Marina 55: 1–17.

Reynolds, C. S., A. E. Irish & J. A. Elliott, 2001. The ecological basis for simulating phytoplankton responses to environmental change (PROTECH). Ecological Modelling 140: 271–291.

Reynolds, C. S., V. Huszar, C. Kruk, L. Naselli-Flores & S. Melo, 2002. Towards a functional classification of the freshwater phytoplankton. Journal of Plankton Research 24: 417–428.

Rodrigues, L. C., B. M. Pivato, L. C. G. Vieira, V. M. Bovo-Scomparin, J. C. Bortolini, A. Pineda & S. Train, 2018. Use of phytoplankton functional groups as a model of spatial and temporal patterns in reservoirs: a case study in a reservoir of central Brazil. Hydrobiologia 805: 147–161.

Rojo, C., 2021. Community assembly: perspectives from phytoplankton's studies. Hydrobiologia 848: 31–52.

Rojo, C. & M. Álvarez-Cobelas, 2003. Are there steady-state phytoplankton assemblages in the field? Hydrobiologia 502: 3–12.

Round, F. E., R. M. Crawford & D. G. Mann, 1990. Diatoms: Biology and Morphology of the Genera, Cambridge University Press, Cambridge.

Rousso, B. Z., E. Bertone, R. Stewart & D. P. Hamilton, 2020. A systematic literature review of forecasting and predictive models for cyanobacteria blooms in freshwater lakes. Water Research 182: 115959.

Ruttner-Kolisko, A., 1977. Suggestions for biomass calculation of planktonic rotifers. Algological Studies/archiv Für Hydrobiologie 8: 71–76.

Salmaso, N. & J. Padisák, 2007. Morpho-Functional Groups and phytoplankton development in two deep lakes (Lake Garda, Italy and Lake Stechlin, Germany). Hydrobiologia 578: 97–112.

Salmaso, N., L. Naselli-Flores & J. Padisák, 2015. Functional classifications and their application in phytoplankton ecology. Freshwater Biology 60: 603–619.

Southwood, T. R. E., 1977. Habitat, the templet for ecological strategies? Journal of Animal Ecology 46: 336–365.

Strickland, J. D. H. & T. R. Parsons, 1965. A Manual of Sea Water Analysis, Fisheries Research Board of Canada Bulletin, Ottawa.

Townsend, C., S. Dolédec & M. Scarsbrook, 1997. Species traits in relation to temporal and spatial heterogeneity in streams: a test of habitat templet theory. Freshwater Biology 37: 367–387.

Utermöhl, H., 1958. Zur Vervollkommnung der quantitativen Phytoplankton-Methodik. Internationalen Vereinigung Für Theoretische Und Angewandte Limnologie Mitteilungen 9: 1–38.

Valderrama, J. C., 1981. The simultaneous analysis of total nitrogen and total phosphorus in natural waters. Marine Chemistry 10: 109–122.

Wehr, J. D., R. G. Sheath & J. P. Kociolek, 2015. Freshwater Algae of North America: Ecology and Classification, Elsevier, Academic Press, San Diego.

Wilson, A. E., O. Sarnelle & A. R. Tillmanns, 2006. Effects of cyanobacterial toxicity and morphology on the population growth of freshwater zooplankton: meta-analyses of laboratory experiments. Limnology and Oceanography 51: 1915–1924.

Wood, S. N., 2004. Stable and efficient multiple smoothing parameter estimation for generalized additive models. Journal of the Royal Statistical Society 99: 673–686.

Wood, S. N., 2011. Fast stable restricted maximum likelihood and marginal likelihood estimation of semiparametric generalized linear models. Journal of the Royal Statistical Society: Series B (Statistical Methodology) 73: 3–36.